IOP Publishing and International Atomic Energy Agency Nuclear Fusion
Nucl. Fusion **52** (2012) 094020 (12pp) doi:10.1088/0029-5515/52/9/094020

Adiabatic description of long range frequency sweeping

R.M. Nyqvist[1], **M.K. Lilley**[2] **and B.N. Breizman**[3]

[1] Department of Earth and Space Science, Chalmers University of Technology, SE-412 96 Göteborg, Sweden
[2] Physics Department, Imperial College, London, SW7 2AZ, UK
[3] Institute for Fusion Studies, The University of Texas at Austin, Austin, Texas 78712, USA

Received 22 December 2011, accepted for publication 19 March 2012
Published 3 September 2012
Online at stacks.iop.org/NF/52/094020

Abstract
A theoretical framework is developed to describe long range frequency sweeping events in the 1D electrostatic bump-on-tail model with fast particle sources and collisions. The model includes three collision operators (Krook, drag (dynamical friction) and velocity space diffusion), and allows for a general shape of the fast particle distribution function. The behaviour of phase space holes and clumps is analysed in the absence of diffusion, and the effect of particle trapping due to separatrix expansion is discussed. With a fast particle distribution function whose slope decays above the resonant phase velocity, hooked frequency sweeping is found for holes in the presence of drag collisions alone.

(Some figures may appear in colour only in the online journal)

1. Introduction

Driven kinetic systems arise naturally far away from thermodynamic equilibrium, and magnetically confined plasmas typically exhibit a wide variety of instabilities that need to be treated kinetically [1]. For example, in externally heated plasmas, fast ions often excite Alfvénic waves capable of degrading energetic ion confinement [2, 3]. The role of dissipation in such systems is far from trivial. Away from the instability threshold, the nonlinear mode evolution consists of an initial saturation followed by a gradual decay [4]. The near-threshold regime, however, exhibits spontaneous formation of coherent phase space structures (holes and clumps) in the fast particle distribution function, which corresponds to the transformation from unstable plasma eigenmodes to energetic particle modes (EPMs) [5] with time dependent mode frequencies [6, 7]. These commonly observed frequency sweeping events [8–11] reflect the tendency for experimental plasmas to persist in near-threshold configurations.

Near the instability threshold, fast particle sources and collisions, which act to restore the unstable fast particle distribution function, compete with the distortion of the distribution function due to the wave field. This interplay results in a nonlinear mode behaviour which differs significantly from the evolution in the collisionless limit. Initial studies revealed a tendency for Krook type collisions [12] and velocity space diffusion [13] to suppress holes and clumps, leading to the conception that frequency sweeping events should not be observed at 'high collisionality'. Recent work [14], however, has shown that the presence of drag (dynamical friction for fast particles) allows holes and clumps to form even in the collisional regime. This has been demonstrated in nonlinear 1D simulations of the bump-on-tail instability [15], which capture the essential features of resonant particle physics in more general multidimensional problems, since particle motion is known to be effectively one dimensional in the vicinity of an isolated nonlinear resonance [13, 16].

The simulations also revealed that the presence of drag in the collisional relaxation of the resonant particles gives rise to asymmetric frequency sweeping, with e.g. steady state and hooked hole behaviours [15]. These features resemble observations from several experiments (see e.g. [17]), which emphasizes the importance of drag for the understanding of frequency sweeping modes. The aforementioned simulations are however limited to short range frequency sweeping, during which the linear mode structure is preserved. In contrast, long range frequency sweeping involves significant changes in the mode structure, which affect the observed sweeping rates [9, 11, 18]. Long range frequency sweeping in the absence of fast particle collisions was recently described in [19].

In this article, we develop a framework that generalizes the formalism of [19] to include fast particle sources and collisions, and to allow for a general shape of the fast particle equilibrium distribution function. As will be shown, the latter modification provides an extension of the analysis in [19] to the case of upsweeping holes, for which the presence of drag in the fast particle collision operator naturally causes hooked frequency

sweeping. The article is organized in the following way: in section 2, we present the bump-on-tail model considered throughout this article, and in section 3 we trim the model to focus on long range sweeping. Section 4 is devoted to the special case of non-diffusive fast particle collisions, and a simple and efficient top-hat model is developed, for which numerical results are presented in section 6. In section 5, we analyse the effect of particle trapping on the wave evolution. Finally, section 7 contains a discussion of the model itself and the presented results.

2. Bump-on-tail model

Motivated by observations of frequency sweeping events in toroidal plasmas, we investigate a perturbation with a prescribed spatial period λ. We consider an electrostatic wave in a 1D plasma with the following three particle species: (1) static ions; (2) cold background electrons with density n_e and perturbed fluid velocity v_e; (3) a small population of fast electrons, which are treated kinetically. The cold electrons respond linearly to the wave field and are subject to weak collisions with collision frequency $2\gamma_d$. The model also includes fast particle sources and collisional relaxation processes, acting to establish a spatially uniform equilibrium distribution function $F_0(v)$, whose velocity gradient provides a linear instability drive with growth rate γ_L.

The starting set of equations is then given by the linearized fluid and continuity equations for the cold electrons, i.e.

$$\frac{\partial v_e}{\partial t} = -\frac{1}{m_e}\frac{\partial U}{\partial x} - 2\gamma_d v_e \tag{1a}$$

and

$$\frac{\partial \delta n_e}{\partial t} = -n_{e0}\frac{\partial v_e}{\partial x}, \tag{1b}$$

where $n_e = n_{e0} + \delta n_e$, the Poisson equation

$$\frac{\partial^2 U}{\partial x^2} = -\frac{e^2}{\epsilon_0}[\delta n_e + \delta n_f], \tag{1c}$$

and a kinetic equation,

$$\frac{\partial f}{\partial t} + v\frac{\partial f}{\partial x} - \frac{1}{m_e}\frac{\partial U}{\partial x}\frac{\partial f}{\partial v} = \mathfrak{C}(f), \tag{1d}$$

describing the evolution of the fast electron distribution function f. Here, the electrostatic potential ϕ of the wave is represented by the potential energy $U \equiv -|e|\phi$, and the perturbed fast electron density is given by

$$\delta n_f = \int (f - F_0)\,\mathrm{d}v. \tag{2}$$

Note that, due to conservation of the total number of particles in the separate fast and cold electron species, we must have

$$\langle \delta n_f \rangle_\lambda = \langle \delta n_e \rangle_\lambda = 0, \tag{3}$$

where $\langle \ldots \rangle_\lambda$ denotes an average over the wavelength λ. Finally, the appropriate fast electron collision operator (cf [14]) is written as

$$\mathfrak{C}(f) = -\beta(f - F_0) + \frac{\alpha^2}{k}\frac{\partial}{\partial v}(f - F_0) + \frac{\nu^3}{k^2}\frac{\partial^2}{\partial v^2}(f - F_0), \tag{4}$$

where $k \equiv 2\pi/\lambda$ is the wavenumber. In (4), Coulomb collisions are modelled by a combination of velocity space diffusion (third term) and a drag/slowing down operator (second term), with effective collision rates $\nu(v)$ and $\alpha(v)$, respectively. The first term is the Krook operator. It annihilates $f - F_0$ at the rate $\beta(v)$, and can serve as a convenient tool for mocking up the effect of the more demanding velocity space diffusion operator. It should also be pointed out that in (4), particle sources and sinks are expressed in terms of the equilibrium distribution function $F_0(v)$.

Equations (1*a*)–(1*d*) describe the system in full generality, including e.g. the process of hole and clump formation (cf [6, 7, 15]). The present investigation, however, is focused on long range frequency sweeping of already established phase space structures, which occurs on a time scale much longer than the bounce period τ_B of resonant electrons trapped in the wave field. The perturbation of interest is then a single travelling wave with spatial period λ and slowly evolving structure. Following the formalism of [19], we represent the perturbed potential energy as

$$U = U(x - s(t); t), \tag{5}$$

where the wave phase velocity $\dot{s}(t)$ changes slowly in time. Here, U is periodic in its first argument, describing fast oscillations at the frequency $\omega \equiv k\dot{s}$ of the dominant Fourier harmonic, and slowly varying with respect to its second argument, describing the evolution of the mode amplitude and structure. More formally, we invoke the adiabatic ordering

$$\left[\frac{\mathrm{d}\ln\omega_B}{dt}, \frac{\mathrm{d}\ln\dot{s}}{\mathrm{d}t}\right] \ll \omega_B \sim \gamma_L \sim \gamma_d \ll \omega, \tag{6}$$

where the bounce frequency $\omega_B = 2\pi/\tau_B$ serves as a measure of the wave amplitude. In this limit, U corresponds to a slowly evolving BGK wave [20], and the description of the fast particles simplifies considerably due to the phase mixed nature of their distribution function.

3. Adiabatic approximation

In the presence of the wave field, the electron motion is governed by the lab frame Hamiltonian

$$\mathcal{H} = \frac{p^2}{2m_e} + U(x - s(t); t), \tag{7}$$

which contains the fast time scale associated with the wave frequency through the potential U. It is natural, however, to use a coordinate system moving with the phase velocity of the wave, thus removing the fast time scale from consideration. The canonical transformation to the wave frame coordinates

$$z = x - s(t), \qquad p_z = p, \tag{8}$$

is achieved by means of the generating function

$$\Phi_1(x, p_z; t) = [x - s(t)]\,p_z + \frac{m_e}{2}\int^t \left(\dot{s}(t')\right)^2 \mathrm{d}t'. \tag{9}$$

At any given moment, the contours of the transformed Hamiltonian (cf [19])

$$\mathcal{H}_z = \frac{[p - m_e\dot{s}(t)]^2}{2m_e} + U(z; t) \tag{10}$$

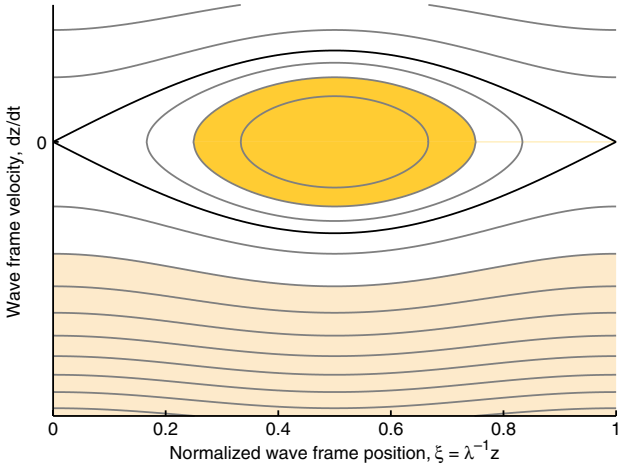

Figure 1. Phase space plot of trapped and passing electron orbits in the wave frame. Each line shows a constant energy trajectory, and the areas of the two shaded regions represent examples of trapped (dark area) and passing (bright area) electron adiabatic invariants.

defines a separatrix in (z, p) phase space centred around $p = m_e\dot{s}$, which separates passing electrons (with wave frame energy $\mathcal{E}_z > U_{max}$) from trapped electrons (satisfying $\mathcal{E}_z < U_{max}$). As seen from (10), $\mathcal{H}_z$ is a function of time, so $\mathcal{E}_z$ is not a conserved quantity. However, there are convenient adiabatic invariants for the trapped and passing electrons, given by the phase space areas bounded by the instantaneous contours of the wave frame Hamiltonian $\mathcal{H}_z$ (see figure 1).

Physically, the separatrix can be viewed as a rigid boundary. As the phase velocity of the wave changes, the trapped electrons are convected along in phase space while the passing electrons flow around the moving separatrix. The coherent motion of the trapped electrons results from the conservation of their adiabatic invariant, whereas the passing electrons are forced to skim the separatrix due to incompressibility of phase space. In total, the process results in (1) a discontinuity in the fast electron distribution function at the separatrix; (2) a release of fast electron kinetic energy. In the presence of fast electron collisions or when the mode structure is evolving slowly, however, the picture is somewhat altered. The separatrix is then more like a porous membrane that allows particles to enter and leave the trapping region, so that the trapped electron distribution function will evolve over time.

In general, all fast electron trajectories are perturbed by the wave field, and so contribute to the perturbed density. However, due to the steep gradient of the distribution function near the separatrix as compared with the ambient distribution (which remains close to the equilibrium slope), the largest part of the perturbed density derives from the trapped particles. When calculating the fast electron perturbed density, we therefore approximate the perturbed distribution function as vanishing outside the separatrix. The effect of the passing electrons then enters as a boundary condition on the trapped electron distribution function, ensuring that $f = F_0$ at the separatrix. On the other hand, all fast electrons contribute to conserve the total number of particles, so we must always make sure to impose $\langle \delta n_f \rangle_\lambda = 0$.

In sections 3.1–3.3, we show how the adiabatic ordering (6) simplifies the treatments of the fast electron distribution function, the wave field and the mode frequency sweeping, respectively.

3.1. Fast electron dynamics

For the purpose of describing the trapped electrons, we adopt the lowest order trapped electron adiabatic invariant (cf [21])

$$J\left(\mathcal{E}_z; t\right) \equiv \frac{\sqrt{2m_e}}{\pi} \int_{z_*}^{\lambda - z_*} \sqrt{\mathcal{E}_z - U\left(z; t\right)}\, \mathrm{d}z \tag{11}$$

as an action variable. Here, the integration limits are the trapped electron turning points, found by solving $\mathcal{E}_z = U(z_*; t)$. The corresponding canonical transformation is defined by the generating function (cf [22])

$$\Phi_2\left(z, J; t\right) = m_e\dot{s}z + \sqrt{2m_e} \int_{z_*}^{z} \sqrt{\mathcal{E}_z\left(J; t\right) - U\left(z'; t\right)}\, \mathrm{d}z', \tag{12}$$

where $\mathcal{E}_z(J; t)$ is defined implicitly by (11). In terms of Φ_2, the canonical angle becomes

$$\theta = \frac{\partial \Phi_2}{\partial J} = \frac{2\pi}{\tau_B}\sqrt{\frac{m_e}{2}} \int_{z_*}^{z} \frac{\mathrm{d}z'}{\sqrt{\mathcal{E}_z\left(J; t\right) - U\left(z'; t\right)}}, \tag{13}$$

where the instantaneous trapped electron bounce period is

$$\tau_B\left(J; t\right) = 2\pi \frac{\partial J}{\partial \mathcal{E}_z} = \sqrt{2m_e} \int_{z_*}^{\lambda - z_*} \frac{\mathrm{d}z}{\sqrt{\mathcal{E}_z\left(J; t\right) - U\left(z; t\right)}}, \tag{14}$$

and the Hamiltonian transforms into

$$\mathcal{H}_{new}\left(\theta, J; t\right) = \mathcal{E}_z\left(J; t\right) + \frac{\partial \Phi_2}{\partial t}, \tag{15}$$

where only the latter part on the right-hand side depends on the angle. Then

$$\dot{J} = -\frac{\partial \mathcal{H}_{new}}{\partial \theta} = -\frac{\partial}{\partial \theta}\frac{\partial \Phi_2}{\partial t} \tag{16}$$

and

$$\dot{\theta} = \frac{\partial \mathcal{H}_{new}}{\partial J} = \omega_B + \frac{\partial}{\partial J}\frac{\partial \Phi_2}{\partial t}, \tag{17}$$

so that the trapped electron kinetic equation reads

$$\frac{\partial f}{\partial t} + \omega_B\frac{\partial f}{\partial \theta} + \frac{\partial f}{\partial \theta}\frac{\partial}{\partial J}\frac{\partial \Phi_2}{\partial t} - \frac{\partial f}{\partial J}\frac{\partial}{\partial \theta}\frac{\partial \Phi_2}{\partial t} = \mathfrak{C}(f). \tag{18}$$

With the adiabatic ordering, we expect the wave to evolve on a slow time scale τ_s, much longer than the bounce period τ_B. We can then expand f in powers of the small parameter

$$\epsilon \equiv \tau_B/\tau_s, \tag{19}$$

and to lowest order we find that (18) becomes

$$\frac{\partial f_0}{\partial \theta} = 0. \tag{20}$$

To lowest order, f is then a function of merely J and t. That is, $f_0 = \langle f \rangle_B$, where the bounce average is defined as

$$\langle \ldots \rangle_B \equiv \frac{1}{2\pi} \int_0^{2\pi} \cdots\, \mathrm{d}\theta. \tag{21}$$

To next order in ϵ, the trapped electron kinetic equation reads

$$\frac{\partial f_0}{\partial t} + \omega_B \frac{\partial f}{\partial \theta} - \frac{\partial f_0}{\partial J}\frac{\partial}{\partial \theta}\frac{\partial \Phi_2}{\partial t} = \mathfrak{C}(f_0). \tag{22}$$

Since f and Φ_2 are both periodic in θ, the second and third terms on the left-hand side of (22) vanish upon application of the bounce average (21), while the first term becomes

$$\frac{\partial f_0}{\partial t} = \frac{\partial \delta f}{\partial t} + \frac{\mathrm{d}F_0(\dot{s})}{\mathrm{d}t}. \tag{23}$$

Here,

$$\delta f \equiv f_0 - \langle F_0 \rangle_B, \tag{24}$$

which by assumption vanishes outside the separatrix. Also, we have assumed that F_0 varies slowly enough with v to be regarded as linear throughout the narrow separatrix region, so that $\langle F_0 \rangle_B = F_0(\dot{s})$ for the trapped fast electrons. The bounce average of the collision operator on the right-hand side of (22) is derived in appendix A. The resulting kinetic equation for the trapped fast electrons reads

$$\frac{\partial\, \delta f}{\partial t} = -\frac{\mathrm{d}F_0}{\mathrm{d}t} - \beta\, \delta f - \frac{\alpha^2}{k}\left.\frac{\mathrm{d}F_0}{\mathrm{d}v}\right|_{v=\dot{s}} + m_e \frac{\nu^3}{k^2}\frac{\partial}{\partial J}\left[J \frac{\mathrm{d}J}{\mathrm{d}\mathcal{E}_z}\frac{\partial\, \delta f}{\partial J}\right]. \tag{25}$$

Note that in applying the bounce average to the collision operator on the right-hand side of (22), the collision frequencies β, α and ν have been assumed to vary slowly with v, so that they can be evaluated at $v = \dot{s}$.

3.2. Wave structure

The adiabatic ordering allows us to simplify the relations (1*a*) and (1*b*). To lowest order, we neglect the effect of the friction force $F_{fr} = -2\gamma_d m_e v_e$ on the background electrons, as well as the slow time variation of U, v_e and δn_e, as compared with the mode frequency ω. We then find that v_e and δn_e are linearly related to U as (cf [19])

$$v_e = \frac{U}{m_e \dot{s}}, \tag{26a}$$

$$\delta n_e = n_{e0}\frac{U}{m_e \dot{s}^2}. \tag{26b}$$

In order to arrive at (26*a*) and (26*b*), we have used (3), assumed that $\langle v_e \rangle_\lambda = 0$, and we have chosen the gauge so that

$$\langle U \rangle_\lambda = 0. \tag{27}$$

The Poisson equation (1*c*) can then be written as

$$\frac{\partial^2 U}{\partial z^2} + \frac{\omega_p^2}{\dot{s}^2}U = -\frac{e^2}{\epsilon_0}\left[\int \delta f\, \mathrm{d}v - \left\langle \int \delta f\, \mathrm{d}v \right\rangle_\lambda\right], \tag{28}$$

where we have transformed to the wave frame and δf, as defined by (24), is determined by (25). The average on the right-hand side of (28) is subtracted in order to conserve the total number of fast electrons, effectively taking into account the small deviation of f from F_0 outside the separatrix. Note that due to the periodicity of U, equation (28) shows that any change in the phase velocity $\dot{s}$ must necessarily be associated with a change in δf. Moreover, as $\dot{s}$ shifts from $\dot{s}_0$ at the initial resonance, the potential U develops a structure different from the cosine obtained in the limit $\delta f \to 0$.

3.3. Frequency sweeping

In the adiabatic regime, the wave lasts much longer than the resistive damping time γ_d^{-1}. The power dissipated in the cold electron background due to the friction force, i.e.

$$Q = 2\gamma_d m_e n_{e0}\int_0^\lambda v_e^2\, \mathrm{d}z = \frac{2\gamma_d n_{e0}}{m_e \dot{s}^2}\langle U^2 \rangle_\lambda, \tag{29}$$

must then be balanced by the power released from the fast electrons during the slow mode evolution. This power balance condition allows the phase velocity of the wave to be determined as a function of time in the following way: if the separatrix is narrow, the lowest order change in fast electron kinetic energy density due to the flow of passing fast electrons around the separatrix can be calculated as

$$\delta\mathcal{E}_p = -m_e\, \dot{s}\, \delta\dot{s}\, \langle F_0 \rangle_B \int_{-v_s}^{v_s} \mathrm{d}v, \tag{30}$$

where v_s labels the fast electron velocity at the separatrix. Note that $\langle F_0 \rangle_B$ should be evaluated using a passing electron trajectory rather than a trapped one, but at the separatrix the results are identical. Similarly, the lowest order change in kinetic energy density among the trapped electrons as the wave changes its phase velocity is

$$\delta\mathcal{E}_t = m_e\, \dot{s}\, \delta\dot{s}\int_{-v_s}^{v_s} f_0\, \mathrm{d}v. \tag{31}$$

The total change in fast electron kinetic energy over one wavelength is then

$$\delta\mathcal{E}_k = \int_0^\lambda [\,\delta\mathcal{E}_p + \delta\mathcal{E}_t]\, \mathrm{d}z = m_e\, \dot{s}\, \delta\dot{s}\int_0^\lambda\int \delta f\, \mathrm{d}v\, \mathrm{d}z, \tag{32}$$

and the power released by the fast particles as the separatrix travels in phase space becomes

$$-\frac{\delta\mathcal{E}_k}{\delta t} = -m_e\, \dot{s}\, \frac{\mathrm{d}\dot{s}}{\mathrm{d}t}\int_0^\lambda\int \delta f\, \mathrm{d}v\, \mathrm{d}z. \tag{33}$$

A similar calculation can be carried out to account for the flow of passing particles around the separatrix due to drag [15]. Effectively, drag modifies the sweeping rate, and the total power balance condition becomes

$$m_e\, \dot{s}\left(\frac{\mathrm{d}\dot{s}}{\mathrm{d}t} + \frac{\alpha^2}{k}\right)\int_0^\lambda\int \delta f\, \mathrm{d}v\, \mathrm{d}z = \frac{2\gamma_d n_{e0}\lambda}{m_e \dot{s}^2}\langle U^2 \rangle_\lambda. \tag{34}$$

3.4. Dimensionless variables

In the subsequent analysis we use dimensionless phase space coordinates

$$\xi \equiv \lambda^{-1} z, \tag{35a}$$

$$u \equiv \phi^{-1}(v - \dot{s}), \tag{35b}$$

and dimensionless time

$$\tau \equiv \frac{8}{3\pi}\phi^2\, \dot{s}_0^{-2}\, \gamma_{L0} t. \tag{35c}$$

We also define the dimensionless quantities

$$\mathcal{U} \equiv m_e^{-1}\phi^{-2}U, \tag{35d}$$

$$\mathcal{E} \equiv m_e^{-1}\phi^{-2}\mathcal{E}_z = \frac{u^2}{2} + \mathcal{U}, \tag{35e}$$

$$\mathcal{J} \equiv \frac{\pi^2}{4} m_e^{-1}\phi^{-1}\lambda^{-1}J, \tag{35f}$$

and

$$\delta\mathcal{F} \equiv \left[\dot{s}_0 \left.\frac{\mathrm{d}F_0}{\mathrm{d}v}\right|_{v=\dot{s}_0}\right]^{-1} \delta f, \tag{35g}$$

$$\rho \equiv \left[\left.\frac{\mathrm{d}F_0}{\mathrm{d}v}\right|_{v=\dot{s}_0}\right]^{-1} \left.\frac{\mathrm{d}F_0}{\mathrm{d}v}\right|_{v=\dot{s}}. \tag{35h}$$

In these expressions, $\dot{s}_0 \equiv \dot{s}(t=0)$ is the initial phase velocity, $\omega_p = k\dot{s}_0$ is the plasma frequency,

$$\gamma_{L0} = \omega_p \frac{\pi}{2n_{e0}} \dot{s}_0^2 \left.\frac{\mathrm{d}F_0}{\mathrm{d}v}\right|_{v=\dot{s}_0} \tag{36}$$

is the initial linear growth rate, and the dimensionless collision rates are given by

$$\widetilde{\beta} \equiv \frac{2}{\pi}\phi^{-3}\dot{s}_0^3 \frac{\beta}{\omega_p}, \tag{37a}$$

$$\widetilde{\alpha}^2 \equiv \frac{2}{\pi}\phi^{-3}\dot{s}_0^3 \frac{\alpha^2}{\omega_p^2}, \tag{37b}$$

$$\widetilde{\nu}^3 \equiv \frac{3\pi}{8}\left(\frac{3\pi^2}{16}\right)^2 \phi^{-2}\dot{s}_0^2 \frac{\nu^3}{\gamma_{L0}^3}, \tag{37c}$$

where

$$\phi \equiv \frac{16}{3\pi^2}\dot{s}_0 \frac{\gamma_{L0}}{\omega_p}. \tag{38}$$

The trapped electron kinetic equation then reads

$$\frac{\partial\,\delta\mathcal{F}}{\partial\tau} + \widetilde{\beta}\,\delta\mathcal{F} = -\rho\left[\frac{\mathrm{d}}{\mathrm{d}\tau}\left(\frac{\dot{s}}{\dot{s}_0}\right) + \widetilde{\alpha}^2\right] + \widetilde{\nu}^3 \frac{\partial}{\partial\mathcal{J}}\left[\mathcal{J}\frac{\partial\mathcal{J}}{\partial\mathcal{E}}\frac{\partial\,\delta\mathcal{F}}{\partial\mathcal{J}}\right], \tag{39}$$

accompanied by the boundary condition

$$\delta\mathcal{F}(\mathcal{J}_S) = 0, \tag{40}$$

where

$$\mathcal{J}_S = \frac{\pi}{2\sqrt{2}}\int_0^1 \sqrt{\mathcal{U}_{max} - \mathcal{U}}\,\mathrm{d}\xi \tag{41}$$

is the value of $\mathcal{J}$ that labels the separatrix. The Poisson equation (28) takes the form

$$\frac{\partial^2\mathcal{U}}{\partial\xi^2} + 4\pi^2\left(\frac{\dot{s}_0}{\dot{s}}\right)^2\mathcal{U} = -\frac{3\pi^3}{2}\left[\int \delta\mathcal{F}\,\mathrm{d}u - \left\langle\int \delta\mathcal{F}\,\mathrm{d}u\right\rangle_\lambda\right], \tag{42}$$

and the power balance condition becomes

$$\frac{\mathrm{d}}{\mathrm{d}\tau}\left(\frac{\dot{s}}{\dot{s}_0}\right) + \widetilde{\alpha}^2 = -2\frac{\gamma_d}{\gamma_{L0}}\left(\frac{\dot{s}_0}{\dot{s}}\right)^3 \left\langle\int \delta\mathcal{F}\,du\right\rangle_\lambda^{-1} \int_0^1 \mathcal{U}^2\mathrm{d}\xi. \tag{43}$$

Since $\delta\mathcal{F} = \delta\mathcal{F}(\mathcal{J};\tau)$, with $\mathcal{J} = \mathcal{J}(\mathcal{E}_z;\tau)$, is symmetric around $u = 0$, we can furthermore rewrite the integral appearing in (42) and (43) as

$$\int \delta\mathcal{F}\,\mathrm{d}u = -2\sqrt{2}\int_{\mathcal{J}(\mathcal{E}=\mathcal{U})}^{\infty} \sqrt{\mathcal{E}(\mathcal{J}) - \mathcal{U}}\,\frac{\partial\,\delta\mathcal{F}}{\partial\mathcal{J}}\,\mathrm{d}\mathcal{J}, \tag{44}$$

where an integration by parts has been performed.

Thus, in the adiabatic approximation, evolving hole/clump BGK modes are described self-consistently by the kinetic equation (39), the Poisson equation (42) and the power balance (43), which are to be solved for $\delta\mathcal{F}$, $\mathcal{U}$ and $\dot{s}/\dot{s}_0$.

4. Top-hat model

Holes and clumps are formed within a narrow region of phase space centred at the phase velocity $\dot{s}_0$ of the linear wave, and the frequency sweeping begins after the trapped fast electrons have become well phase mixed [6]. We can therefore approximate $\delta\mathcal{F}$ as initially flat inside the separatrix. Moreover, in the absence of diffusion, the kinetic equation (39) contains no derivatives with respect to $\mathcal{J}$, so $\delta\mathcal{F}$ will remain flat unless the separatrix grows. In this case, we model $\delta\mathcal{F}$ by taking

$$\delta\mathcal{F}(\mathcal{J};\tau) = h(\tau)\left[\Theta(\mathcal{J}) - \Theta(\mathcal{J} - \mathcal{J}_S(\tau))\right], \tag{45}$$

which describes a column in $\mathcal{J}$-space, whose width decreases as the separatrix shrinks and whose height can be found by integrating the kinetic equation

$$\frac{\mathrm{d}h}{\mathrm{d}\tau} + \widetilde{\beta}h = -\rho\left[\frac{\mathrm{d}}{\mathrm{d}\tau}\left(\frac{\dot{s}}{\dot{s}_0}\right) + \widetilde{\alpha}^2\right]. \tag{46}$$

Thus, h varies in time as the phase velocity changes or due to Krook and drag collisions (which preserve the flatness of the distribution inside the separatrix). Moreover, the *top-hat* distribution (45) permits the integral in (42) and (43) to be evaluated analytically as

$$\int \delta\mathcal{F}\,\mathrm{d}u = 2\sqrt{2}\,h\sqrt{\mathcal{U}_{max} - \mathcal{U}}, \tag{47}$$

which in turn enables an analytical solution of the Poisson equation in terms of $\dot{s}$. Following the method outlined in [19], we obtain

$$\mathcal{U} = \frac{\pi^2}{2}\frac{(\dot{s}/\dot{s}_0)^4 h^2}{\cos^2\eta}\left\{\frac{1+2\cos^2\eta}{2} - \frac{3}{4}\frac{\sin 2\eta}{\eta} - [\cos\eta - \cos(\eta(2\xi-1))]^2\right\}, \tag{48}$$

where $\eta \equiv \pi\dot{s}_0/2\dot{s}$. For the maximum value of the potential we find

$$\mathcal{U}_{max} = \frac{\pi^2}{4}\frac{(\dot{s}/\dot{s}_0)^4 h^2}{\cos^2\eta}\left\{\sin^2\eta + 3\cos^2\eta\left[1 - \frac{\sin\eta}{\eta\cos\eta}\right]\right\}, \tag{49}$$

and the value of the action at the separatrix becomes

$$\mathcal{J}_S = \frac{\pi}{2}(\dot{s}/\dot{s}_0)^3 h[\eta - \tan\eta]. \tag{50}$$

Substitution of these results into the power balance condition (43) gives the frequency sweeping rate

$$\frac{\mathrm{d}}{\mathrm{d}\tau}\left(\frac{\dot{s}}{\dot{s}_0}\right) = \frac{\gamma_d}{\gamma_{L0}}\frac{\pi^4}{2^5}\frac{M_1}{M_2}h^2\left(\frac{\dot{s}}{\dot{s}_0}\right)^2 - \widetilde{\alpha}^2, \tag{51}$$

with

$$M_1 = \frac{1}{2} + \frac{11\sin 4\eta}{24\eta} + 8\cos^2\eta - \left(\frac{3\sin 2\eta}{2\eta}\right)^2 - \frac{2\sin 2\eta}{3\eta}, \tag{52a}$$

$$M_2 = \cos^3\eta[\sin\eta - \eta\cos\eta]. \tag{52b}$$

Thus, with a top-hat distribution of the form (45), the wave evolution is found by simply integrating the system of ordinary differential equations (46) and (51) to determine h and $\dot{s}$. This model was previously analysed in [19] for the case of a collisionless clump. The generalization presented here describes the evolution and long range frequency sweeping of holes and clumps in the presence of fast electron sources and collisions. Note, however, that as the phase velocity of clumps approaches $\dot{s}_0/2$, the potential (48) develops new minima centred at $\xi = 0$ and $\xi = 1$. This is not accounted for in the approximation (45), so the model breaks down at approximately $\dot{s} = \dot{s}_0/2$.

Formally, the top-hat model applies to holes and clumps whose separatrices do not expand. To determine whether the separatrix will initially shrink or grow, we expand $\mathcal{J}_S$ as given by (50) in the initially small quantity $\delta \equiv (\dot{s}-\dot{s}_0)/\dot{s}_0$. To second order in δ, the effect of Krook collisions can be neglected in (46). Drag, however, can not be neglected, and we find that

$$h = -\delta\left[1 + \left(\frac{K}{2} + \frac{4}{\pi}\frac{\gamma_{L0}}{\gamma_d}\widetilde{\alpha}^2\right)\delta\right] + \mathcal{O}\left(\delta^3\right), \tag{53}$$

where

$$K \equiv \left[\dot{s}_0 \left.\frac{dF_0}{dv}\right|_{v=\dot{s}_0}\right]^{-1} \dot{s}_0^2 \left.\frac{d^2F_0}{dv^2}\right|_{v=\dot{s}_0}. \tag{54}$$

Using (53) in (50), $\mathcal{J}_S$ can be expanded as

$$\mathcal{J}_S = 1 + \left[4 - \left(\frac{\pi}{2}\right)^2 + \frac{K}{2} + \frac{4}{\pi}\frac{\gamma_{L0}}{\gamma_d}\widetilde{\alpha}^2\right]\delta + \mathcal{O}\left(\delta^2\right), \tag{55}$$

meaning that the initial separatrix evolution is sensitive to the second derivative of the equilibrium distribution function and the rate of drag. From (55), it is seen that the separatrix shrinks initially for upsweeping phase space holes when

$$K \leqslant K_c \equiv -2\left[4 - \left(\frac{\pi}{2}\right)^2 + \frac{4}{\pi}\frac{\gamma_{L0}}{\gamma_d}\widetilde{\alpha}^2\right], \tag{56}$$

and for downsweeping phase space clumps when $K \geqslant K_c$, so the top-hat model applies to holes in the former case and clumps in the latter case. Moreover, when the equilibrium distribution function is fine tuned so that $K = K_c$, neither holes nor clumps will initially grow.

In fact, (50) can be solved for the critical column height needed to keep $\mathcal{J}_S$ constant throughout the entire evolution. This height is given by

$$h_c = \frac{2}{\pi\left(\dot{s}/\dot{s}_0\right)^3}[\eta - \tan\eta]^{-1}, \tag{57}$$

where $\mathcal{J}_S(\tau = 0) = 1$ has been substituted, and it has been plotted as a function of $\dot{s}/\dot{s}_0$ in figure 2. Note that without fast electron collisions, i.e. in the limit $\widetilde{\beta} = \widetilde{\alpha} = \widetilde{\nu} = 0$,

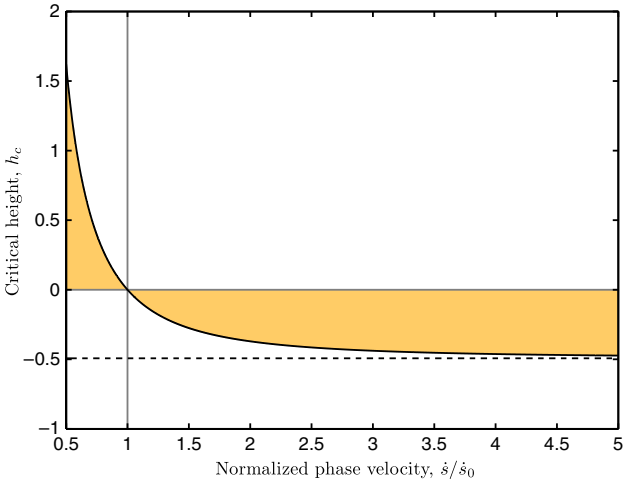

Figure 2. Critical height of hole/clump needed to keep the value of the action at the separatrix constant throughout the evolution. A necessary condition for a non-expanding separatrix is that h is always bounded to the shaded region. For large phase velocities, h_c approaches the asymptotic value $-3(2/\pi)^4$.

this critical height corresponds to having an equilibrium distribution function on the form

$$F_0(\dot{s}) = F_0(\dot{s}_0) - \dot{s}_0 \left.\frac{dF_0}{dv}\right|_{v=\dot{s}_0} h_c, \tag{58}$$

with

$$\rho = -\dot{s}_0\frac{dh_c}{d\dot{s}}. \tag{59}$$

In the presence of Krook and drag collisions, there is no simple connection between h and F_0, so in general one has to evolve the mode to see whether or not the separatrix expands. However, since the effect of Krook in (46) is to decrease $|h|$, any F_0 that results in a non-expanding separatrix in the collisionless limit will yield a sub-critical evolution of h in the presence of Krook as well (including e.g. the critical distribution given in (58)). Drag, on the other hand, acts to reduce clump heights and deepen holes at the rate $\rho\widetilde{\alpha}^2$. Hence, in the presence of drag, any F_0 that results in a non-expanding separatrix in the collisionless limit will yield a sub-critical evolution of h for clumps, but not necessarily for holes.

5. Particle trapping

As previously discussed, the shape of the equilibrium distribution function will in general force either holes or clumps to initially expand. When this happens, new particles are captured from the ambient equilibrium slope and brought inside the separatrix, so that the trapped electron distribution function develops a gradient in the proximity of the separatrix. Thus, as in the presence of diffusive fast electron collisions, the top-hat approximation breaks down, and a new procedure is needed to solve the kinetic equation (39) for the trapped electron distribution function.

A less demanding (but still instructive) step is to investigate the wave evolution in the presence of a *ring* (see figure 3) that extends inwards from the separatrix, and on which the trapped electron distribution takes on the value of the

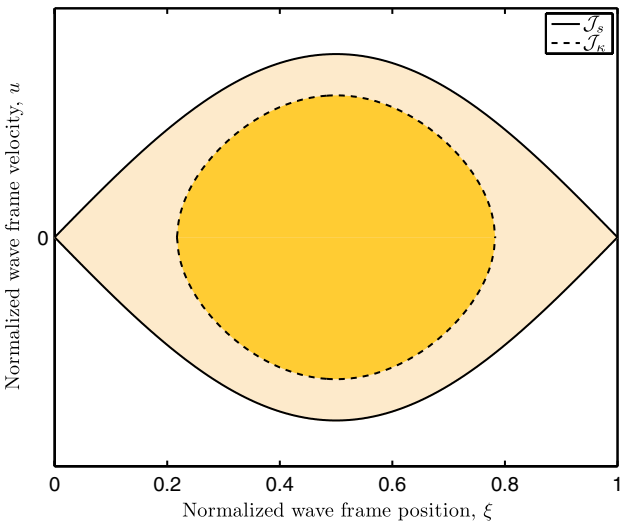

Figure 3. Hole/clump structure with ring. The hole/clump has the height h in the dark, central region, i.e. from 0 to $\mathcal{J}_\kappa$. In the brighter ring, i.e. the subregion from $\mathcal{J}_\kappa$ to $\mathcal{J}_S$, it has vanishing height.

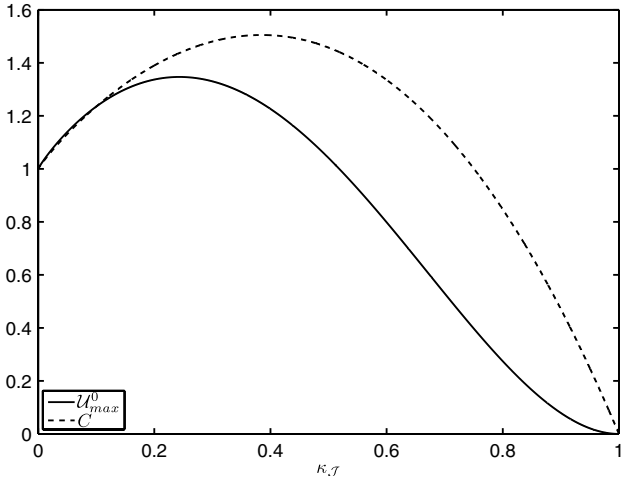

Figure 4. With larger and larger fractional ring areas, the initial amplitude of holes and clumps first increases, then reaches a maximum, and finally decreases. The frequency sweeping coefficient C behaves in a similar manner.

ambient distribution function. For this purpose, we develop a perturbative approach described in appendix B, which we use to calculate $\mathcal{U}_{\max}$ during the early evolution stage when the mode structure is approximately sinusoidal. In figure 4, the initial amplitude $\mathcal{U}^0_{\max} \equiv \mathcal{U}_{\max}(\tau = 0)$ is plotted as a function of fractional ring area $\kappa_\mathcal{J}$, defined as

$$\kappa_\mathcal{J} \equiv \frac{\mathcal{J}_S - \mathcal{J}_\kappa}{\mathcal{J}_S}, \tag{60}$$

with $\mathcal{J}_\kappa$ the value of the action at the inner ring boundary. This curve reproduces an earlier result obtained in [23] by a different method. It is noteworthy that $\mathcal{U}^0_{\max}$ is non-monotonic: it initially increases with $\kappa_\mathcal{J}$ and then passes through a maximum. So, as $\mathcal{J}_S$ increases due to finite δ in (55), the effect of particle trapping tends to accelerate the growth even further. In appendix B we also calculate the initial frequency sweeping as a function of $\kappa_\mathcal{J}$. In physical units, one finds (cf (B.16))

$$\omega = \omega_p \pm \frac{16}{3\pi^2}\sqrt{\frac{2}{3}}\, C\,(\kappa_\mathcal{J})\, \gamma_{L0}\sqrt{\gamma_d t}, \tag{61}$$

where $C(\kappa_\mathcal{J})$ has been plotted alongside $\mathcal{U}^0_{\max}$ in figure 4. For a ringless top-hat structure we have $C(\kappa_\mathcal{J} = 0) = 1$, which reproduces the previously obtained square root frequency sweeping [6]. As seen from figure 4 and (61), the initial sweeping rate has non-monotonic dependence on $\kappa_\mathcal{J}$, with a maximum when $C \approx 1.5$ at $\kappa_\mathcal{J} \lesssim 0.4$.

In an attempt to mimic the effect of particle trapping, we can use the perturbative model to evolve a hole from a ringless state (with a completely empty separatrix region) at the resonant frequency ω_p, to a configuration with larger $\mathcal{J}_S$ (and hence a ring) at a slightly larger frequency $\omega = \omega_p(1+\delta)$ with $\delta \ll 1$. Requiring the system to evolve adiabatically, we demand that as the separatrix expands in accordance with (55) and a ring emerges, $\mathcal{J}_\kappa$ must always remain at the value of $\mathcal{J}_S(\tau = 0) = 1$. Thus, setting $\mathcal{J}_\kappa = 1$ in the expression (B.9) for $\mathcal{J}_\kappa$, and substituting the expression for the initial amplitude (B.13), we arrive at the equation

$$2h\frac{\dot{s}^2}{\dot{s}^2 - \dot{s}_0^2}\left\{\frac{\kappa-1}{2}K\left(\sqrt{\frac{\kappa+1}{2}}\right) - \kappa E\left(\sqrt{\frac{\kappa+1}{2}}\right)\right\} \times \left\{\frac{\kappa-1}{2}K\left(\sqrt{\frac{\kappa+1}{2}}\right) + E\left(\sqrt{\frac{\kappa+1}{2}}\right)\right\} = 1, \tag{62}$$

which is to be solved for κ. Here, K and E are the complete elliptic integrals of the first and second kind, respectively, and κ labels the inner ring boundary in terms of particle energy (see appendix B). Substituting $\dot{s} = \dot{s}_0(1+\delta)$ and (53) for the height in (62), we find $\kappa = 0.8782$ and $\kappa_\mathcal{J} = 0.1005$, which indicates that the inital separatrix growth triggers a quick transition into a state where the trapping region comprises a significant ring. This observation is consistent with a conclusion made in [23] about an instability during which the mode evolves non-adiabatically. However, the work in [23] does not take into account the full $\dot{s}$-dependence in the Poisson equation. In particular, the multiplicative factor $(\dot{s}^2 - \dot{s}_0^2)/\dot{s}^2$ in (B.2) is approximated by δ, which leads to shortcomings in the analysis of the mode amplitude evolution. Note that the above procedure can also be used to show that the initial, non-adiabatic evolution can be avoided if the holes and clumps are set up with initial rings.

6. Effect of collisions and equilibrium profile on mode evolution

In this section we present spectrograms obtained by means of the top-hat model presented in section 4. All calculations are performed using $\gamma_{L0} = \gamma_d$. Clumps are run with a linear equilibrium distribution function F_0, and for holes we model F_0 as a quadratic function of $\dot{s}$, with $K = K_c$ as given by (56) and $\widetilde{\alpha} = 0.8$. The resulting equilibrium profile (see figure 5) constitutes a non-monotonic bump-on-tail distribution, with a maximum at $\dot{s} = \dot{s}_0(1 - 1/K_c) \approx 1.2\dot{s}_0$.

Figure 6 displays the frequency sweeping of holes and clumps in the collisionless limit $\widetilde{\beta} = \widetilde{\alpha} = 0$. It is seen that the top-hat model results deviate from the symmetric square

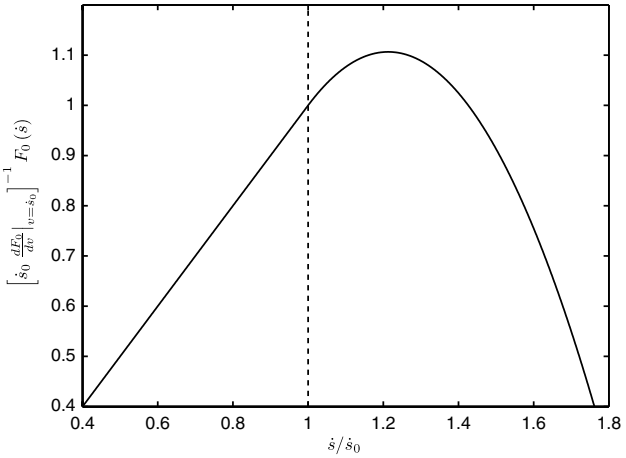

Figure 5. Normalized fast electron equilibrium distribution function. The vertical, dashed line marks the initial phase velocity $\dot{s}_0$ of holes and clumps.

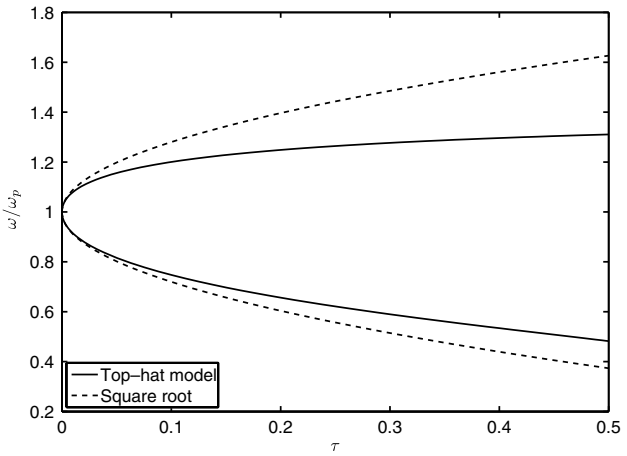

Figure 6. Frequency evolution for holes and clumps in the absence of collisions.

root sweeping (61) predicted if the mode amplitudes are held fixed. For the downsweeping clump, the deviation from the square root derives from the evolution of the mode structure, whereas the larger abberance in the hole frequency sweeping is due to both the evolving mode structure and the nonlinear equilibrium profile.

Krook and drag collisions enrich the observed behaviours of holes and clumps. To separate the effects of Krook and drag, we first show in figures 7 and 8 how finite $\widetilde{\beta}$ affects the frequency sweeping of holes and clumps and the evolution of $\mathcal{U}_{\max}$ for holes in the absence of drag (the effect of finite $\widetilde{\beta}$ on the evolution of $\mathcal{U}_{\max}$ for clumps is very similar to the result for holes presented in figure 8). For both holes and clumps, it is seen that finite $\widetilde{\beta}$ decreases the frequency sweeping rates, and that these reductions correlate with the increased rates at which the Krook collisions are abating $\mathcal{U}_{\max}$ by diminishing the depth/height of the holes and clumps, as previously discussed at the end of section 4.

Drag, on the other hand, affects the evolution through both (46) and (51). Hence, it imposes an additional frequency sweeping rate $-\widetilde{\alpha}^2$, but it also acts asymmetrically to deepen holes and diminish clumps, thus tending to increase/decrease

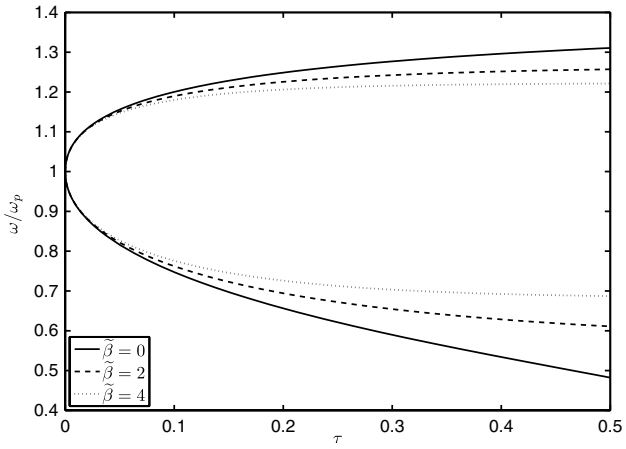

Figure 7. Frequency evolution of holes and clumps with $\widetilde{\alpha} = 0$ and $\widetilde{\beta}$ ranging from 0 to 4.

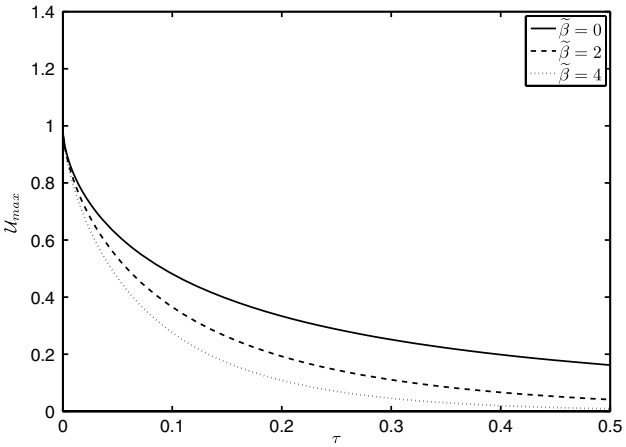

Figure 8. Amplitude evolution of hole with $\widetilde{\alpha} = 0$ and $\widetilde{\beta}$ ranging from 0 to 4. The amplitude evolution of the corresponding clump behaves in a qualitatively similar manner.

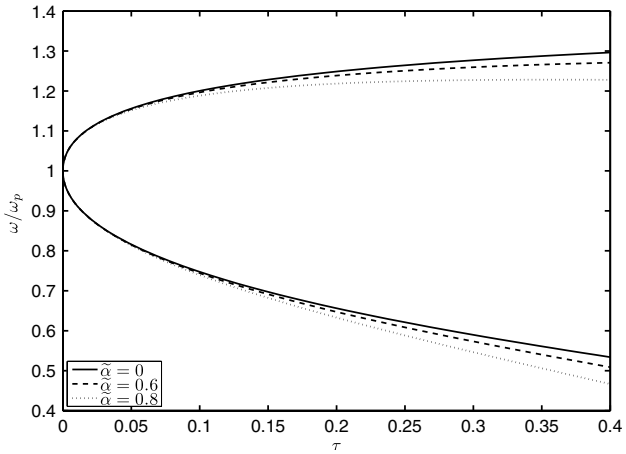

Figure 9. Frequency evolution of holes and clumps with $\widetilde{\beta} = 0$ and $\widetilde{\alpha}$ ranging from 0 to 0.8.

the respective hole/clump mode amplitudes. For holes, the sweeping rate in figure 9 is seen to decrease with increasing $\widetilde{\alpha}$ even though the rate of decay of the amplitude is also lowered, as seen in figure 10. The opposite applies for clumps, where the

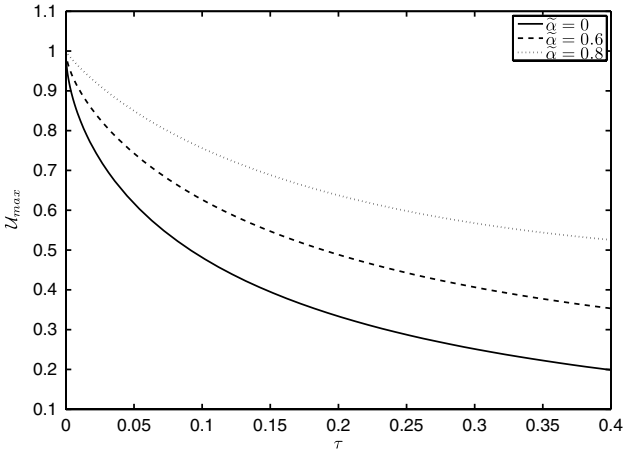

Figure 10. Amplitude evolution of hole with $\widetilde{\beta} = 0$ and $\widetilde{\alpha}$ ranging from 0 to 0.8.

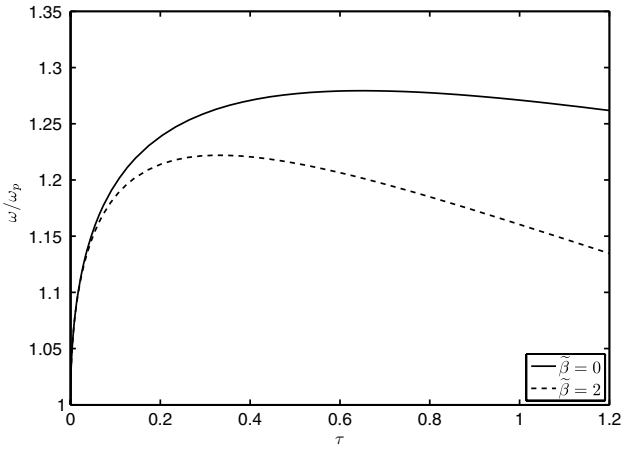

Figure 12. Frequency evolution of hooking holes with $\widetilde{\alpha} = 0.4$ and $\widetilde{\beta}$ ranging from 0 to 2.

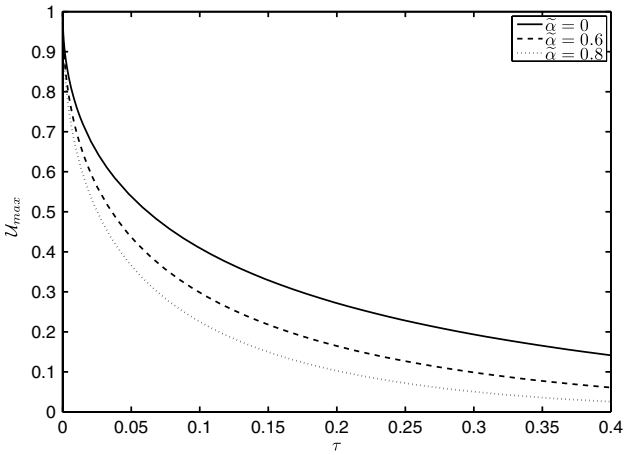

Figure 11. Amplitude evolution of clump with $\widetilde{\beta} = 0$ and $\widetilde{\alpha}$ ranging from 0 to 0.8.

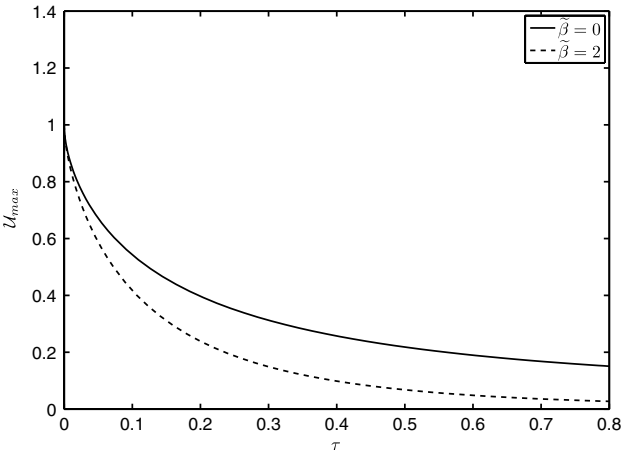

Figure 13. Amplitude evolution of hooking holes with $\widetilde{\alpha} = 0.4$ and $\widetilde{\beta}$ ranging from 0 to 2.

frequency sweeping rate turns out to increase with $\widetilde{\alpha}$, and the sweeping can become almost linear at low mode amplitudes, as seen in figures 9 and 11. Note, however, that in the limit $\tau \to 0$, all the curves in figures 7 and 9 tend to the square root results, confirming the picture that neither collisions nor the nonlinear equilibrium slope significantly alters the initial frequency sweeping.

If run a little longer, it is evident that the hole frequency sweeping in the presence of drag is non-monotonic (see figure 12): these so called *hooks* sweep up in frequency, until eventually reaching a maximum where the two terms on the right-hand side of (51) balance and the frequency evolution is reversed. As $\widetilde{\alpha}$ increases, the turning point is reached sooner in the evolution and at lower frequency. The same type of *hooks* are also found with a combination of Krook collisions and drag (dashed line in figure 12), where the former act to attenuate the mode quicker (see figure 13), so that the turning point is reached sooner in the evolution and at lower frequency.

7. Discussion and conclusions

The present investigation is motivated by multiple observations of long range frequency sweeping events in plasmas [9, 11, 18]. The corresponding theoretical concept is that wave excitation in the near-threshold regime leads to spontaneous formation of phase space structures, i.e. groups of fast particles moving coherently in phase space and capable of producing a signal with frequency deviating from that of the linearly excited mode. For such structures to survive in the presence of dissipation, they need to travel in fast particle phase space, which produces a frequency sweep in the observed signal. This mechanism has been thoroughly investigated for the 1D bump-on-tail model (including the present work), and the results are conceptually applicable to more general systems, provided that the wave-particle resonances are well separated in phase space.

In tokamak plasmas, toroidal Alfvén eigenmodes (TAEs) commonly serve as seeds for long range frequency sweeping, when such modes are excited by energetic particles. The observed evolution of TAEs range from steady saturation to pitchfork splitting [24], spectral broadening [25] and frequency sweeping events [8–11], sometimes with significant deviation from the excitation frequency towards or even into the Alfvén continuum. The relation $\omega \propto \sqrt{t}$ predicted by 1D bump-on-tail theory (cf (61)) has been successfully applied to frequency sweeping TAEs within the Alfvén gap [8]. In a more recent effort to model the mode sweeping beyond the Alfvén gap [26],

continuum damping effectively enhances the dissipation rate, which gives rise to accelerated sweeping. However, a truly consistent description of long range sweeping TAEs has not yet been developed. The challenge is to capture the effect of the resonant particles on the TAE mode structure.

In the light of the above discussion, the presented adiabatic bump-on-tail model constitutes a logical step towards predictive modeling of nonlinear mode evolution in three dimensional experimental configurations. By ignoring the complex hole/clump formation stage, the adiabatic model enables an efficient description of initially prescribed coherent phase space structures on time scales larger than the trapped electron bounce period, and it allows for significant frequency sweeping (on the order of the mode frequency itself) during which the mode structure evolves considerably. In this work, two essential features have been added to the earlier analysis in [19]. First, fast electron sources and collisions (Krook, drag and velocity space diffusion) are introduced through a proper bounce average of the collision operators. Second, the model is designed to allow for a nonlinear slope in the equilibrium distribution function. In particular, the latter property permits an adiabatic description of upward sweeping holes within a simple top-hat model, in cases where the shape of the equilibrium distribution function keeps the mode separatrix from expanding.

The top-hat model results presented in section 6 reveal a new feature of non-monotonic (hooked) frequency sweeping. Hooked frequency sweeping was previously observed for holes during short range frequency sweeping in a linear equilibrium slope, as a result of the interplay between drag and velocity space diffusion [15]. During long range frequency sweeping, however, variation in the slope of the equilibrium distribution function can, in the presence of drag, also produce hooks, as shown in figure 12.

The tendency for fast and sudden growth of the mode amplitude due to particle trapping is an interesting feature where the mode automatically traps extra particles in such a way that the initial state is modified to comprise a ring. This trend was first reported in [23], where adiabatic frequency sweeping was found to terminate for some initial configurations. The presence of this instability and its connection to trapping of passing particles sheds some light on a mysterious numerical enhancement of the frequency sweeping rate obtained in earlier work [15]. It has since then been observed that significant particle trapping was occurring in these investigations, without an obvious physics reason. It is indeed intriguing that the observed numerical enhancement of about 1.4 is attainable with an initial ring, and actually roughly corresponds to the fractional ring area yielding the maximum initial mode amplitude. Further investigations are however necessary to be more conclusive.

Implementation of the physically more relevant situation with diffusive fast electron collisions necessitates solving (39) numerically, which is the aim of future work. Such a fully numerical, kinetic scheme would constitute a more realistic approach, enabling the complete description of particle trapping, and potentially resolve the breakdown due to the formation of new potential minima in the evolving spatial profile of the nonlinear wave.

Acknowledgments

The authors are grateful to M. Lisak for his interest in this work and for his support that made this collaboration possible. This work was funded jointly by the Swedish Research Council, EURATOM and by the US Department of Energy Contract No DE-FG02-04ER54742.

Appendix A. Bounce averaged collision operator

In this section we present derivations of the bounce averages of the Krook, drag and diffusion terms in the lowest order collision operator for the trapped electrons in (25). The calculations are performed by transforming to the action-angle variables defined by (11) and (13). The resulting expressions are then averaged over θ as prescribed by (21), and under the assumption that F_0 and the collision rates β, α and ν are smooth functions of v. Since the trapped electron velocity in the wave frame,

$$v_z \equiv v - \dot{s}, \tag{A.1}$$

satisfies $v_z \ll \dot{s}$, this assumption means that we can regard F_0, β, α and ν as linear throughout the trapping region.

A.1. Krook operator

The Krook term,

$$\mathfrak{C}_{\mathrm{K}}(f_0) = -\beta(f_0 - F_0), \tag{A.2}$$

is easily bounce averaged by direct application of (21). One obtains

$$\langle \mathfrak{C}_{\mathrm{K}}(f_0)\rangle_{\mathrm{B}} = -\beta\delta f, \tag{A.3}$$

where

$$\delta f \equiv f_0 - \langle F_0\rangle_{\mathrm{B}} = f_0 - F_0(\dot{s}). \tag{A.4}$$

A.2. Drag operator

The drag, or slowing down, collision operator is given by

$$\begin{aligned}\mathfrak{C}_{\mathrm{SD}}(f_0) &= -\frac{\alpha^2}{k}\frac{\partial}{\partial v}(f_0 - F_0)\\ &= -\frac{\alpha^2}{k}\left[\frac{\partial J}{\partial v_z}\frac{\partial f_0}{\partial J} - \left.\frac{\mathrm{d}F_0}{\mathrm{d}v}\right|_{v=\dot{s}}\right].\end{aligned} \tag{A.5}$$

Here,

$$\frac{\partial J}{\partial v_z} = \frac{\partial \mathcal{E}_z}{\partial v_z}\frac{\partial J}{\partial \mathcal{E}_z} = m_{\mathrm{e}} v_z \frac{\partial J}{\partial \mathcal{E}_z}, \tag{A.6}$$

where $J = J(\mathcal{E}_z; t)$, so we obtain

$$\langle \mathfrak{C}_{\mathrm{SD}}(f_0)\rangle_{\mathrm{B}} = -\frac{\alpha^2}{k}\left[m_{\mathrm{e}}\langle v_z\rangle_{\mathrm{B}}\frac{\partial J}{\partial \mathcal{E}_z}\frac{\partial f_0}{\partial J} - \left.\frac{\mathrm{d}F_0}{\mathrm{d}v}\right|_{v=\dot{s}}\right]. \tag{A.7}$$

For trapped electrons we have $\langle v_z\rangle_{\mathrm{B}} = 0$. Hence,

$$\langle \mathfrak{C}_{\mathrm{SD}}(f_0)\rangle_{\mathrm{B}} = -\frac{\alpha^2}{k}\left.\frac{\mathrm{d}F_0}{\mathrm{d}v}\right|_{v=\dot{s}}. \tag{A.8}$$

A.3. Diffusion operator

We first use repeatedly equation (A.6) to transform the velocity derivatives in the diffusion operator. We then obtain

$$\begin{aligned}\mathfrak{C}_{\mathrm{D}}(f_0) &= \frac{\nu^3}{k^2}\frac{\partial^2}{\partial v^2}(f_0 - F_0)\\ &= \frac{\nu^3}{k^2}\frac{\partial}{\partial v_z}\left[m_{\mathrm{e}} v_z \frac{\partial J}{\partial \mathcal{E}_z}\frac{\partial f_0}{\partial J}\right]\\ &= \frac{\nu^3}{k^2}\left\{m_{\mathrm{e}}\frac{\partial J}{\partial \mathcal{E}_z}\frac{\partial f_0}{\partial J} + m_{\mathrm{e}}^2 v_z^2 \frac{\partial J}{\partial \mathcal{E}_z}\frac{\partial}{\partial J}\left[\frac{\partial J}{\partial \mathcal{E}_z}\frac{\partial f_0}{\partial J}\right]\right\},\end{aligned} \tag{A.9}$$

where only the factor v_z^2 needs to be bounce averaged. For trapped electrons,

$$\langle v_z^2\rangle_{\mathrm{B}} = \frac{\omega_{\mathrm{B}}}{m_{\mathrm{e}}} J, \tag{A.10}$$

with $\omega_{\mathrm{B}} = (\partial J/\partial \mathcal{E}_z)^{-1}$. We can then combine the two terms on the right-hand side of (A.9) into

$$\langle \mathfrak{C}_{\mathrm{D}}(f_0)\rangle_{\mathrm{B}} = m_{\mathrm{e}}\frac{\nu^3}{k^2}\frac{\partial}{\partial J}\left[J\frac{\partial J}{\partial \mathcal{E}_z}\frac{\partial f_0}{\partial J}\right]. \tag{A.11}$$

Finally, by noting that for trapped electrons

$$\frac{\partial}{\partial v}\langle F_0\rangle_{\mathrm{B}} = \frac{\partial}{\partial v}F_0(\dot{s}) = 0, \tag{A.12}$$

we arrive at

$$\langle \mathfrak{C}_{\mathrm{D}}(f_0)\rangle_{\mathrm{B}} = m_{\mathrm{e}}\frac{\nu^3}{k^2}\frac{\partial}{\partial J}\left[J\frac{\partial J}{\partial \mathcal{E}_z}\frac{\partial\, \delta f}{\partial J}\right]. \tag{A.13}$$

Appendix B. Perturbative approach

In this section, we present a perturbative description of the mode evolution during the early phase, when the phase velocity of the wave is close to $\dot{s}_0$ and the mode structure is approximately sinusoidal. For this purpose, we rewrite the Poisson equation (42) as

$$\frac{\partial^2 \mathcal{U}}{\partial \xi^2} + 4\pi^2 \mathcal{U} = \Psi(\mathcal{U}; \dot{s}), \tag{B.1}$$

where

$$\Psi(\mathcal{U}; r) \equiv 4\pi^2\frac{\dot{s}^2 - \dot{s}_0^2}{\dot{s}^2}\mathcal{U} + \frac{3\pi^3}{2}\left\{\int \delta\mathcal{F}\,\mathrm{d}u - \left\langle \int \delta\mathcal{F}\,\mathrm{d}u\right\rangle_{\lambda}\right\} \tag{B.2}$$

is initially small compared with each of the two terms on the left-hand side of (B.1). Defining

$$\mathcal{U}_0 = A\cos 2\pi\xi \tag{B.3}$$

to be the solution to the equation obtained by setting $\Psi = 0$ in (B.1), the self-adjointness of the linear operator on the left-hand side of (B.1) requires Ψ to be orthogonal to $\mathcal{U}_0$, i.e.

$$\int_0^1 \mathcal{U}_0\,\Psi\,(\mathcal{U}; \dot{s})\,\mathrm{d}\xi = 0. \tag{B.4}$$

Early in the mode evolution, the smallness of Ψ allows us to set $\mathcal{U} \approx \mathcal{U}_0$ in the solvability condition (B.4), which results in an equation for the linear mode amplitude A, namely,

$$\begin{aligned}&2A + 3\sqrt{2}\pi\frac{\dot{s}^2}{\dot{s}^2 - \dot{s}_0^2}\int_0^1 \cos 2\pi\xi\\ &\quad\times\int_{\mathcal{J}(\mathcal{E}=\mathcal{U}_0)}^{\infty}\sqrt{\mathcal{E}(\mathcal{J}) - A\cos 2\pi\xi}\,\frac{\partial\delta\mathcal{F}}{\partial\mathcal{J}}\,\mathrm{d}\mathcal{J}\,\mathrm{d}\xi = 0.\end{aligned} \tag{B.5}$$

This formula can be used together with the kinetic equation (39) and the power balance condition (43) to efficiently evolve holes and clumps during the early stage when $\mathcal{U}$ is approximately sinusoidal, thus replacing the Poisson equation (42).

In particular, equation (B.5) is very convenient for analysing the top-hat model from section 4, since all involved integrals can then be evaluated analytically. It also helps to analyse the case when the trapping region comprises a subregion (a so called *ring*), extending inward from the separatrix, on which the trapped electron distribution function takes on the ambient (passing electron) value. We then have (cf (45))

$$\delta\mathcal{F}\,(\mathcal{J}; \tau) = h\,(\tau)\,[\Theta\,(\mathcal{J}) - \Theta\,(\mathcal{J} - (1 - \kappa_{\mathcal{J}}\,(\tau))\,\mathcal{J}_{\mathrm{S}}\,(\tau))], \tag{B.6}$$

where the fractional ring area is defined as

$$\kappa_{\mathcal{J}} \equiv \frac{\mathcal{J}_{\mathrm{S}} - \mathcal{J}_{\kappa}}{\mathcal{J}_{\mathrm{S}}}. \tag{B.7}$$

In these expressions, the action at the separatrix can be evaluated as

$$\mathcal{J}_{\mathrm{S}} = \frac{\pi}{2\sqrt{2}}\sqrt{A}\int_0^1 \sqrt{1 - \cos 2\pi\xi}\,\mathrm{d}\xi = \sqrt{A}, \tag{B.8}$$

and $\mathcal{J}_{\kappa}$ is the action at the inner boundary of the ring, i.e.

$$\begin{aligned}\mathcal{J}_{\kappa} &= \frac{\pi}{2\sqrt{2}}\sqrt{A}\int_{\frac{1}{2\pi}\arccos\kappa}^{1-\frac{1}{2\pi}\arccos\kappa}\sqrt{\kappa - \cos 2\pi\xi}\,\mathrm{d}\xi\\ &= \sqrt{A}\left\{\frac{\kappa - 1}{2}K\left(\sqrt{\frac{\kappa+1}{2}}\right) + E\left(\sqrt{\frac{\kappa+1}{2}}\right)\right\}.\end{aligned} \tag{B.9}$$

Here, K and E are the complete elliptic integrals of the first and second kind, respectively, and $\kappa \in [-1, 1]$ is defined as

$$\kappa \equiv \mathcal{E}_{\kappa}/A, \tag{B.10}$$

where $\mathcal{E}_{\kappa}$ is the instantaneous energy at the inner ring boundary. A completely empty top-hat structure with $\kappa_{\mathcal{J}} = 0$, i.e. one whose interior takes on the value h on the entire trapping region, is represented by $\kappa = 1$, whereas a completely filled top-hat structure with $\kappa_{\mathcal{J}} = 1$ and $\delta\mathcal{F} = 0$ has $\kappa = -1$. In terms of κ, the fractional ring area reads

$$\kappa_{\mathcal{J}} = 1 + \frac{1 - \kappa}{2}K\left(\sqrt{\frac{\kappa+1}{2}}\right) - E\left(\sqrt{\frac{\kappa+1}{2}}\right). \tag{B.11}$$

With (B.6), we can actually solve explicitly for A. We find that

$$\begin{aligned}&\int_{J(\mathcal{E}=\mathcal{U}_0)}^{\infty}\sqrt{\mathcal{E}(\mathcal{J}) - A\cos 2\pi\xi}\,\frac{\partial\delta\mathcal{F}}{\partial\mathcal{J}}\,\mathrm{d}\mathcal{J}\\ &= -h\sqrt{A}\sqrt{\kappa - \cos 2\pi\xi},\end{aligned} \tag{B.12}$$

so that

$$\sqrt{A} = \frac{3\pi}{\sqrt{2}} h \frac{\dot{s}^2}{\dot{s}^2 - \dot{s}_0^2} \int_{\frac{1}{2\pi}\arccos\kappa}^{1-\frac{1}{2\pi}\arccos\kappa} \cos 2\pi\xi \sqrt{\kappa - \cos 2\pi\xi}\, \mathrm{d}\xi$$
$$= 2h \frac{\dot{s}^2}{\dot{s}^2 - \dot{s}_0^2} \left\{ \frac{\kappa - 1}{2} K\left(\sqrt{\frac{\kappa+1}{2}}\right) - \kappa E\left(\sqrt{\frac{\kappa+1}{2}}\right) \right\} \quad \text{(B.13)}$$

Furthermore, (B.13) may be substituted into the power balance condition and used to calculate the initial frequency sweeping. Doing so yields

$$\frac{\mathrm{d}}{\mathrm{d}\tau}\left(\frac{\dot{s}}{\dot{s}_0}\right) + \tilde{\alpha}^2 = \pi \frac{\gamma_\mathrm{d}}{\gamma_{\mathrm{L}0}} \frac{(\dot{s}/\dot{s}_0)^3 h^2}{\left((\dot{s}/\dot{s}_0)^2 - 1\right)^3} C^2(\kappa), \quad \text{(B.14)}$$

where

$$C^2(\kappa) \equiv \frac{\left[\frac{1-\kappa}{2} K\left(\sqrt{\frac{\kappa+1}{2}}\right) + \kappa E\left(\sqrt{\frac{\kappa+1}{2}}\right)\right]^3}{\frac{\kappa-1}{2} K\left(\sqrt{\frac{\kappa+1}{2}}\right) + E\left(\sqrt{\frac{\kappa+1}{2}}\right)}. \quad \text{(B.15)}$$

During the early evolution stage, h can be approximated using (53). To lowest order in $\delta = (\dot{s} - \dot{s}_0)/\dot{s}_0$, we then find

$$\frac{\dot{s}}{\dot{s}_0} = 1 \pm \sqrt{\frac{\pi}{4}\frac{\gamma_\mathrm{d}}{\gamma_{\mathrm{L}0}}}\, C(\kappa) \sqrt{\tau}. \quad \text{(B.16)}$$

In figure 4 of section 5, $\sqrt{A}$ and C are plotted as functions of $\kappa_\mathcal{J}$.

References

[1] Heidbrink W.W. and Sadler G.J. 1994 *Nucl. Fusion* **34** 535
[2] Fasoli A. 2007 *et al* Progress in the ITER Physics Basis: Chapter 5: Physics of energetic ions *Nucl. Fusion* **47** S264
[3] Wong K.L. *et al* 1991 *Phys. Rev. Lett.* **66** 1874
[4] Berk H.L., Breizman B.N. and Huanchun Ye 1992 *Phys. Rev. Lett.* **68** 3563
[5] Chen L. 1994 *Phys. Plasmas* **1** 1519
[6] Berk H.L., Breizman B.N. and Petviashvili N.V. 1997 *Phys. Lett.* A **234** 213
[7] Berk H.L., Breizman B.N. and Candy J., Pekker M. and Petviashvili N.V. 1999 *Phys. Plasmas* **6** 3102
[8] Pinches S.D., Berk H.L., Gryaznevich M.P., Sharapov S.E. and JET-EFDA Contributors 2004 *Plasma Phys. Control. Fusion* **46** S47
[9] Fredrickson E., Gorelenkov N., Bell R., Menard J., Roquemore A., Kubota S., Crocker N. and Peebles W. 2006 *Nucl. Fusion* **46** S926
[10] Heidbrink W.W., Strait E., Doyle E., Sager G. and Snider R. 1991 *Nucl. Fusion* **31** 1635
[11] Shinohara K. *et al* 2001 *Nucl. Fusion* **41** 603
[12] Berk H.L., Breizman B.N. and Pekker M.S. 1996 *Phys. Rev. Lett.* **76** 1256
[13] Breizman B.N., Berk H.L., Pekker M.S., Porcelli F., Stupakov G.V. and Wong K.L. 1997 *Phys. Plasmas* **4** 1559
[14] Lilley M.K., Breizman B.N. and Sharapov S.E. 2009 *Phys. Rev. Lett.* **102** 195003
[15] Lilley M.K., Breizman B.N. and Sharapov S.E. 2010 *Phys. Plasmas* **17** 092305
[16] Chirikov B.V. 1979 *Phys. Rep.* **52** 263
[17] Berk H.L., Boswell C., Borba D., Figueiredo A., Johnson T., Nave M., Pinches S., Sharapov S.E. and JET-EFDA Contributors 2006 *Nucl. Fusion* **46** S888
[18] Maslovsky D., Levitt B. and Mauel M.E. 2003 *Phys. Plasmas* **10** 1549
[19] Breizman B.N. 2010 *Nucl. Fusion* **50** 084014
[20] Bernstein I.B., Greene J.M. and Kruskal M.D. 1957 *Phys. Rev.* **108** 546
[21] Goldstein H., Poole C. and Safko J. 2002 *Classical Mechanics* (San Fransisco, CA: Addison Wesley)
[22] Cary J.R. and Escande R.T. 1989 *Physica* D **36** 287
[23] Eremin Yu D. and Berk H.L. 2002 *Phys. Plasmas* **9** 772
[24] Fasoli A., Breizman B.N., Borba D., Heeter R.F., Pekker M.S. and Sharapov S.E. 1998 *Phys. Rev. Lett.* **81** 5564
[25] Heeter R.F., Fasoli A.F. and Sharapov S.E. 2000 *Phys. Rev. Lett.* **85** 3177
[26] Wang G. and Berk H.L. 2012 *Commun. Nonlinear Sci. Numer. Simulation* **17** 2179